Global Gene Expression Analysis in *PKCα*$^{-/-}$ Mouse Skin Reveals Structural Changes in the Dermis and Defective Wound Granulation Tissue

Nichola H. Cooper[1,2], Jeya P. Balachandra[1] and Matthew J. Hardman[1]

The skin's mechanical integrity is maintained by an organized and robust dermal extracellular matrix (ECM). Resistance to mechanical disruption hinges primarily on homeostasis of the dermal collagen fibril architecture, which is regulated, at least in part, by members of the small leucine-rich proteoglycan (SLRP) family. Here we present data linking protein kinase C alpha (PKCα) to the regulated expression of multiple ECM components including SLRPs. Global microarray profiling reveals deficiencies in ECM gene expression in PKCα$^{-/-}$ skin correlating with abnormal collagen fibril morphology, disorganized dermal architecture, and reduced skin strength. Detailed analysis of the skin and wounds from wild-type and PKCα$^{-/-}$ mice reveals a failure to upregulate collagen and other ECM components in response to injury, resulting in delayed granulation tissue deposition in PKCα$^{-/-}$ wounds. Thus, our data reveal a previously unappreciated role for PKCα in the regulation of ECM structure and deposition during skin wound healing.

Journal of Investigative Dermatology (2015) **135,** 3173–3182; doi:10.1038/jid.2015.338; published online 24 September 2015

INTRODUCTION

The Protein Kinase C (PKC) family comprises around 15 highly abundant serine/threonine kinase isozymes that participate in a multitude of signaling pathways across numerous tissues (Zeng *et al.*, 2012). Although many PKCs are expressed in the skin, protein kinase C alpha (PKCα) is most abundant and widely distributed. In the epidermis, PKCα has an integral role in regulating keratinocyte terminal differentiation (Matsui *et al.*, 1992; Tibudan *et al.*, 2002; Jerome-Morais *et al.*, 2009) and desmosomal adhesion (Wallis *et al.*, 2000; Kimura *et al.*, 2007; Kimura *et al.*, 2012). Indeed, we have recently shown that PKCα is essential for the timely modulation of epidermal cell–cell adhesion to permit wound re-epithelialization (Thomason *et al.*, 2012). By contrast, and despite widespread dermal expression, the role(s) of PKCα in non-epidermal tissues remain unclear.

Seventy percent of the mammalian dermis is noncellular, and is instead composed of a complex heterogeneous extracellular matrix (ECM). Fibrillar collagens predominate, assembling into large fibril bundles that form a structural meshwork. Collagen proteins undergo extensive post-translation modification (Canty and Kadler, 2005; Gordon and Hahn, 2010) with mature collagen fibril morphology maintained by numerous ECM proteins including the small leucine-rich proteoglycans (SLRPs). SLRPs have wide-ranging biological functions including bone and tooth mineralization, blood vessel viscoelasticity, and, most importantly, maintenance of skin tensile strength (Merline *et al.*, 2009). Their localization and ability to interact with diverse receptors, cytokines, growth factors, and other ECM components permit selective modulation of cell–matrix interactions and signaling. During normal skin homeostasis, dermal ECM turnover is negligible. Indeed, many of the collagen and elastic fibers laid down during development will persist throughout adulthood, gradually accumulating damaging modifications (Naylor *et al.*, 2011). Following injury, however, ECM is rapidly deposited and remodeled, resulting in an imperfect but functional scar (Martin, 1997). In addition, there is evidence that SLRPs are involved in this ECM remodeling in skin and oral mucosa repair and in cutaneous scar formation (Honardoust *et al.*, 2008; Honardoust *et al.*, 2011; Yamanaka *et al.*, 2013; Nikolovska *et al.*, 2014).

We have recently reported a pronounced delay in skin repair in *PKCα*$^{-/-}$ mice. Defects early in re-epithelization lead to a failure to switch desmosomal cell adhesion *in vivo* and a direct delay in keratinocyte migration (Thomason *et al.*, 2012). However, the severity of the *PKCα*$^{-/-}$ wound-healing phenotype led us to predict defects in processes other than re-epithelialization. This prediction is supported by known

[1]*The Healing Foundation Centre, Faculty of Life Sciences, University of Manchester, Manchester, UK and* [2]*Institute of Medical Biology, Epithelial Epigenetics Laboratory, Agency for Science, Technology and Research, Singapore, Singapore*

Correspondence: Matthew J. Hardman, The Healing Foundation Centre, Faculty of Life Sciences, University of Manchester, Oxford Road, Manchester 138648, UK. E-mail: matthew.j.hardman@manchester.ac.uk

Abbreviations: ECM, extracellular matrix; GO, Gene Ontology; KO, knock-out; PKCα, protein kinase C alpha; SLRP, small leucine-rich proteoglycan; WT, wild type

Received 18 March 2015; revised 10 August 2015; accepted 12 August 2015; accepted article preview online 9 September 2015; published online 24 September 2015

functions of PKCs in non-epithelial cell types in non-healing contexts, where they are involved in processes such as proliferation, inflammation, and angiogenesis (Wang and Smart, 1999; Diegelmann and Evans, 2004; Cataisson *et al.*, 2006).

Here we have employed a transcriptional profiling approach to globally characterize the role of PKCα in skin homeostasis and repair. Our data reveal that PKCα deficiency leads to defects in numerous aspects of healing, including ECM matrix remodeling. Intriguingly, in the absence of PKCα, multiple members of the SLRP family are intrinsically misexpressed during skin homeostasis, resulting in abnormal collagen fibril morphology, disorganized collagen matrix, and increased skin fragility. We propose that this phenotype predisposes the *PKCα*$^{-/-}$ mice to skin lesions and biases toward poorer healing via delayed granulation tissue deposition.

RESULTS

Experimental design

The magnitude of the healing delay in *PKCα*$^{-/-}$ mice led us to propose a role for *PKCα* in non-desmosomal aspects of healing and dermal homeostasis (Thomason *et al.*, 2012). To identify these alternative roles we carried out comprehensive microarray profiling of the skin and wounds from *PKCα*$^{-/-}$ and wild-type (WT) mice collected immediately before and 24 hours post wounding (Figure 1). These time points were carefully selected to reveal intrinsic differences (unwounded skin, Figure 1a and b) and early causative changes (24-hour wounds, Figure 1d and g). Crucially, 24 hours post injury precedes overt differences in healing between WT and *PKCα*$^{-/-}$ (Figure 1d and g).

PCA analysis confirmed the robustness of the unfiltered normalized data set (see Materials and Methods) with experimental groups tightly clustering on PC1 (52%; wound) and PC2 (19%; genotype; Supplementary Figure 1 online). Two data sets were generated for subsequent analysis. First, gene expression was directly compared between WT and *PKCα*$^{-/-}$ unwounded skin (Figure 1c and Table 1). Second, gene expression was simultaneously compared between all four groups using analysis of variance (ANOVA) and unsupervised cluster analysis (Figure 1 and 4 and Supplementary Table 1 online). Subsequent quantitative PCR validation was performed on selected genes representing various expression profiles to confirm differences between all four groups (WT and *PKCα*$^{-/-}$ skin and wounds; Supplementary Figure 2 online).

Coordinate changes in ECM genes in the unwounded PKCα$^{-/-}$ skin

Direct comparison of PKCα$^{-/-}$ and WT skin (Figure 1c) revealed a total of 209 differentially (>2-fold) expressed probe sets (54 upregulated and 154 downregulated in *PKCα*$^{-/-}$ vs. WT). Most obvious was the coordinate downregulation of multiple ECM-related genes in the *PKCα*$^{-/-}$ skin. Specifically, expression of the genes encoding the two

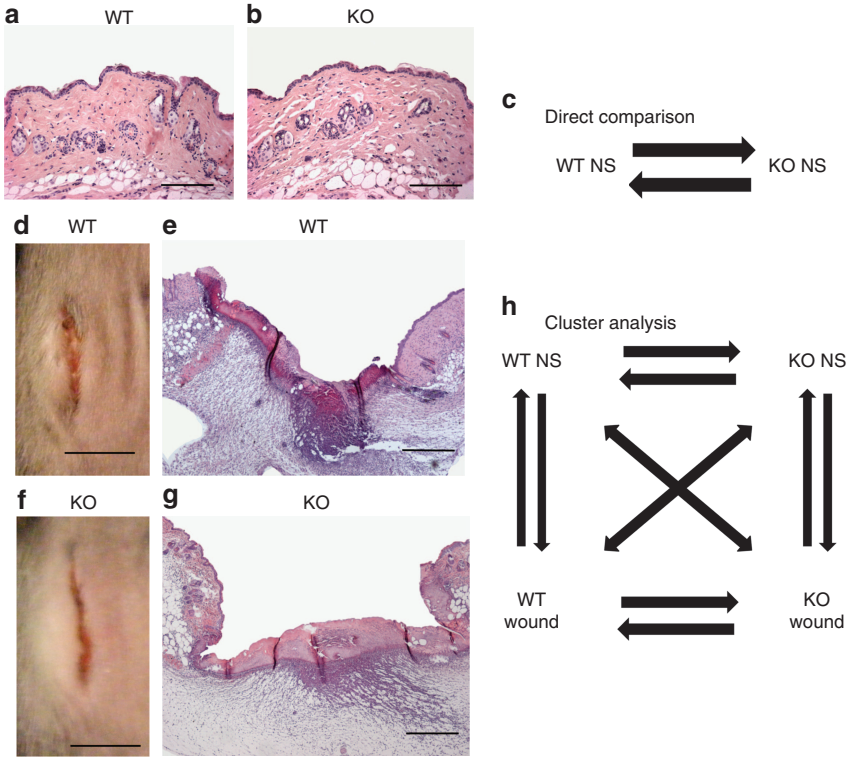

Figure 1. Experimental microarray design. Tissue isolated from WT and KO skin (**a**, **b**) and wounds (24 hours post wounding, **d**–**g**). Microarray analysis was carried out on and two data sets generated from the expression analysis; direct comparison of genes differentially regulated between WT and KO normal skin (**c**) and ANOVA/unsupervised cluster analysis across all experimental groups (**h**). ANOVA, analysis of variance; KO, Knock-out; NS, normal skin; W, wound; WT, wild type.

Table 1. Key genes identified via microarray showing differential expression in PKCα$^{-/-}$ skin compared with wild-type skin[1]

More than 2-fold up in KO skin		More than 2-fold down in KO skin	
Gene name	**Fc**	**Gene name**	**Fc**
Lipocalin 2 (Lcn2)	6.80	*Aquaporin (Aqp4)*	−6.23
Synuclein Alpha (Snca)	6.34	***Osteoglycin (Ogn)***	**−5.92**
RASD family, member 2 (Rasd2)	4.40	*Collagen, type III, alpha 1 (Col3a1)*	−5.54
Defensin beta 6 (Defb6)	3.90	*Collagen, type I, alpha 1 (Col1a1)*	−5.13
Ets homologous factor (Ehf)	3.73	*Thrombospondin 4 (Thbs4)*	−5.00
Polyadenylate binding protein-interacting protein 1 (Paip1)	3.54	*Chemokine (C-C motif) receptor 2 (Ccr2)*	−4.65
Chitinase 3-like 1 (Chi3l1)	3.74	***Lumican (Lum)***	**−4.24**
Musculoskeletal embryonic nuclear protein 1 (Mustn1)	3.18	*Lysyl Oxidase (Lox)*	−4.12
Phenylethanolamine-N-Methytransferase (Pnmt)	3.08	*Collagen, type 5, alpha 1 (Col5a1)*	−2.83
F-box protein 32 (Fbxo32)	3.08	*Collagen, type 5, alpha 2 (Col5a2)*	−2.82
Dishevelled activator of morphogenesis 1(Daam1)	2.69	***Decorin (Dcn)***	**−2.48**
Psoriasis susceptibility 1 candidate 1 (Psors1c2)	2.26	***Biglycan (Bgn)***	**−2.47**
Filamin C gamma (Finc)	2.09	*Elastin (Eln)*	−2.39
Interleukin 1 family member 6 (Il1f6)	2.06	*Friend Leukemia Integration 1 (Fli1)*	−2.15

Abbreviations: KO, Knock-out; PKCα, protein kinase C alpha; WT, wild type.
[1]Direct comparison of genes up- and downregulated in KO compared with WT, genes selected on fold change (>2) and *q*-value (<0.05).

principle skin fibrillar collagen species (Col1a1 and Col3a1) was >5-fold lower in *PKCα*$^{-/-}$. Numerous SLRP family members, such as Osteoglycin, Biglycan, Decorin, and Lumican (highlighted in bold, Table 1), were coordinately downregulated. Interestingly, Lysyl Oxidase (LOX) and Elastin (ELN) showed a >2-fold downregulation in the *PKCα*$^{-/-}$ skin (Table 1), further suggesting a global, intrinsic ECM deficiency. In addition, we also note a coordinate downregulation of numerous ECM components in human dermal fibroblasts upon PKCα inhibition (Gö6976), more pronounced when fibroblasts are treated with transforming growth factor-β1 to stimulate ECM production (Supplementary Figure 3 online).

SLRP downregulation correlates with reduced *PKCα*$^{-/-}$ skin tensile strength

Reduced SLRP gene expression in *PKCα*$^{-/-}$ mice was particularly interesting, as SLRP deficiencies are known to functionally alter the skin (Danielson *et al.*, 1997; Chakravarti *et al.*, 1998; Corsi *et al.*, 2002; Tasheva *et al.*, 2002). Immunoblotting using antibodies specific to a subset of the downregulated SLRPs (lumican, osteoglycin, and biglycan) confirmed reduced protein levels in the *PKCα*$^{-/-}$skin compared with WT (Figure 2a and b). Given that SLRP deficiencies are known to influence the dermal structure and skin integrity, we asked whether similar changes would be present in *PKCα*$^{-/-}$ mice. Transmission electron microscopy imaging of transversely orientated dermal collagen fibrils revealed altered morphology in the *PKCα*$^{-/-}$skin (Figure 2c). Specifically, the range of collagen fibril diameters was greater in the *PKCα*$^{-/-}$skin (20–247 nm) compared with the WT skin (26–182 nm) with increased variance (measure of the data spread; Figure 2d). This inconsistency in fibril diameter inevitably led to increased interfibrillar spacing (arrows; Figure 2c). *PKCα*$^{-/-}$ collagen fibrils were noted to be more irregular in shape than WT fibrils (Figure 2c), implying an increased incidence of lateral fusions, as has been documented previously in SLRP null mice (Danielson *et al.*, 1997; Chakravarti *et al.*, 1998; Corsi *et al.*, 2002; Tasheva *et al.*, 2002).

Skin's tensile strength is maintained, at least in part, by the ordered arrangement of collagen fibril bundles. We thus asked whether the identified changes in the collagen network of the *PKCα*$^{-/-}$ skin would functionally alter skin strength. Comparative tension testing of the WT and *PKCα*$^{-/-}$ skin revealed altered functional properties (Figure 2e and f). When strips of the skin were loaded to failure using a tension-testing apparatus (Intron 3344), stress–strain curves revealed that stress to failure was significantly reduced and was more variable in the skin from *PKCα*$^{-/-}$ (7.75 N) versus WT (9.6 N) mice (Figure 2e and f). Despite the clear difference in skin's tensile strength the elastic modulus, determined as stress: strain from the midpoint of the elastic region of the curve, was not significantly different (data not shown).

Next, we asked whether the altered collagen fibril morphology and experimentally demonstrated reduction in skin's tensile strength in the *PKCα*$^{-/-}$ skin would manifest functionally *in vivo* under normal homeostasis. In fact, from 5 months of age we observed a phenotype of spontaneous skin breaking and wound development in *PKCα*$^{-/-}$ mice (Figure 3). This phenotype was unique to *PKCα*$^{-/-}$ mice seen in 6 out of 26 mice aged to 6 months and beyond. Our co-aged WT mice appeared normal and, indeed, over

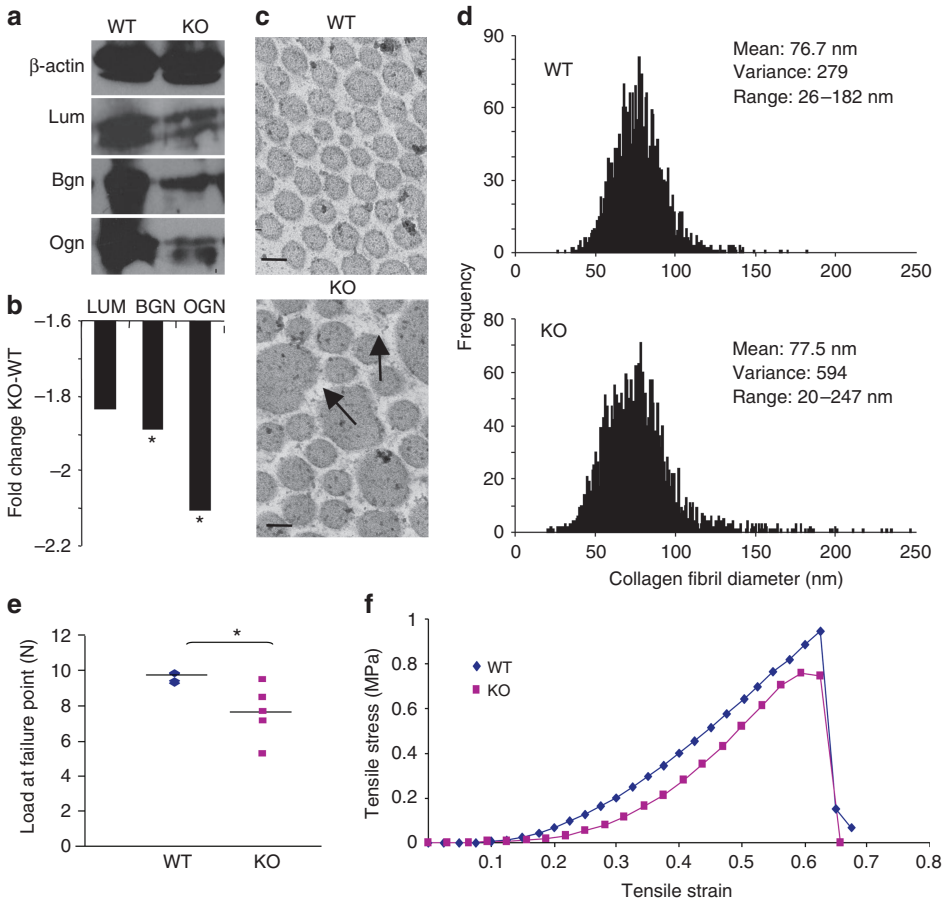

Figure 2. Dermal extracellular matrix (ECM) changes. Immunoblotting reveals reduced SLRP protein expression in the KO skin (**a**, **b**). Transmission electron micrographs depicting dermal collagen fibrils with an increased variance, diameter, and interfibrillar spacing (**c**, arrows) in the KO skin (**c**, **d**). Kolmogorov–Smirnov and F-tests performed on the data distribution suggest that the data are significantly different ($P \leqslant 0.0001$; **d**). Load force at the point of failure was lower in the KO skin compared with WT (**e**). Representative stress–strain curves for the WT and KO skin show reduced tensile strength in the KO skin loaded to failure at a constant rate of 20 mm min^{-1}. Curves taken from samples with median failure load (**f**). Scale bar = 100 nm (**c**); $n = 2{,}300$–$2{,}600$ fibrils taken from three mice (**c**); $n = 4$–5 6-week-old female mice (**e**, **f**). $^*P \leqslant 0.05$ (**e**), $P \leqslant 0.0001$ (**d**). KO, Knock-out; SLRP, small leucine-rich proteoglycan; WT, wild type.

extensive prior WT ageing studies we have never observed spontaneous skin breaking, even at 32 months of age. Interestingly, Masson's Trichrome and immunofluorescence revealed that observed changes in collagen gene expression in the young *PKCα* −/− skin (Table 1) led to a clear reduction in collagen protein in both non-lesional and lesional skin from mature *PKCα*$^{-/-}$ mice (Figure 3e and l). Despite no changes in skin thickness, the phenotype manifests itself only after mice mature to ~5 months of age; younger control mice (6 weeks) appear normal (Figure 3a and d). Indeed, histologically lesional *PKCα*$^{-/-}$ skin was severely perturbed, with an absent epidermis, abnormal dermal architecture (Figure 3k and l), and extensive inflammatory cell infiltration (data not shown).

Gene profiling reveals the complexity of *PKCα* functions during wound healing

To obtain a more detailed picture of PKCα-dependent gene regulation/interaction in response to injury, we performed ANOVA/unsupervised clustering of microarray data across all experimental groups (i.e., skin and wounds; Figure 1h). Unsupervised clustering of the full enriched data set produced a total of 16 experimental clusters, perfectly mirroring hypothetical cluster profiles (Supplementary Table 1 and Supplementary Figure 4 online). In total, 2,682 genes were regulated by both genotype and wounding, either independently (12.5%) or through interaction (19.3%; Supplementary Figure 5 online). Selected experimental clusters are shown in Figure 4a and d, along with corresponding cluster-specific over-represented Gene Ontology (GO) groups and key genes from each cluster. Many genes were similarly up- or down-regulated following wounding in both WT and *PKCα*$^{-/-}$ (Figure 4a and b), in association with known wound-related GO groupings such as "immune response". In line with our direct PKCα$^{-/-}$ versus WT skin comparison (Table 1), a number of genes were regulated by genotype alone (Figure 4c and Supplementary Table 1 online), including the GO groups "collagen" and "wnt signaling". Whereas Wnts and PKCs

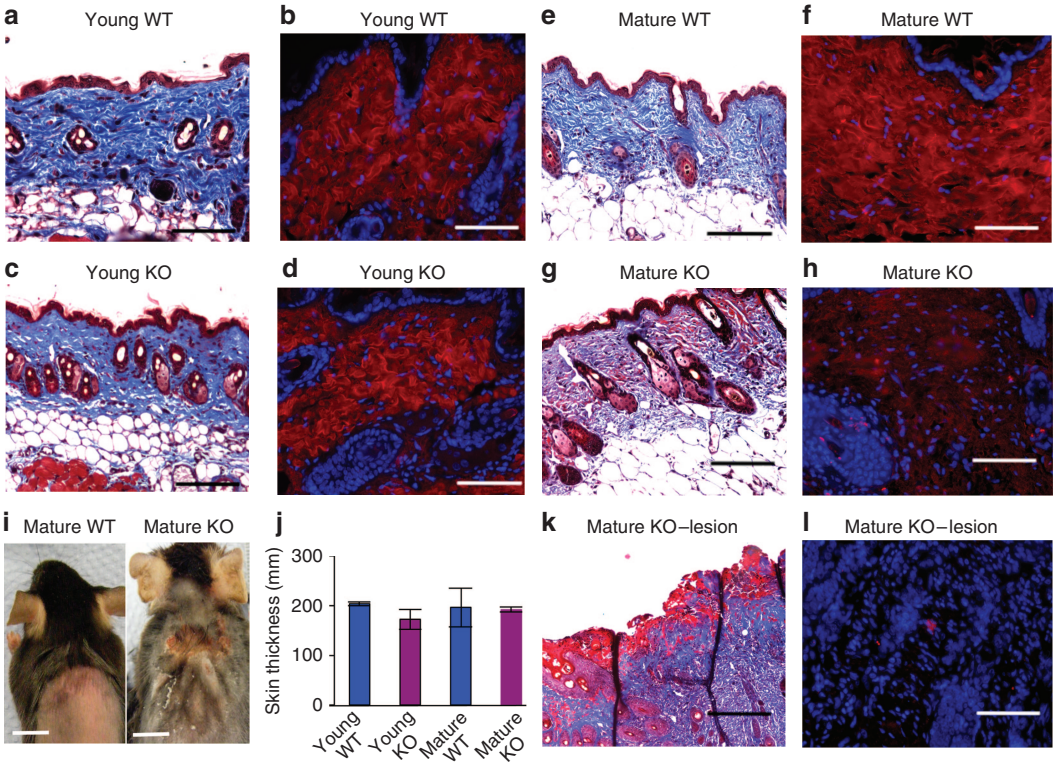

Figure 3. Altered dermal architechture in Knock-out (KO) skin. Masson's Trichrome staining and collagen 1 immunofluorescence reveal a comparable dermal architecture and ECM composition in young WT and KO skin (**a**–**d**) but highlight differences in the mature skin (**h**–**k**). In the KO skin (**g**, **h**), despite no differences in skin thickness (**j**), age results in a reduced dermal collagen content (blue staining, Masson's Trichrome) and reduced collagen I expression compared with age-matched WT (**h, i**). In addition, the KO skin is more prone to the development of spontaneous wounds (**e**, **f**). Masson's Trichome and collagen I immunofluorescence (red, Collagen I; blue, 4',6-diamidino-2-phenylindole) on the lesional KO skin (**j**, **k**) reveal a clear wound area and an absence of Collagen I expression (**k**, **l**). $N = 6$ WT and KO; Scale bars = 1 cm (**a**, **b**), 500 μm (**c**, **d**). WT, wild type.

have been linked previously (e.g., Dissanayake and Weeraratna, 2008; Luna-Ulloa *et al.*, 2011; Hernandez-Maqueda *et al.*, 2013), an association in the context of skin biology is to our knowledge previously unreported and worthy of future investigation. A number of clusters containing genes with an interaction profile were identified, i.e., differentially regulated by wounding between genotypes (Figure 4d and Supplementary Table 1 online). Cluster D was particularly interesting, containing genes upregulated upon injury in WT but not in *PKCα*$^{-/-}$ wounds. GO analysis reveals that *PKCα*$^{-/-}$ mice fail to induce "Collagen" and "Immune Response" genes upon injury. We observe that *PKCα*$^{-/-}$ shows no significant inflammatory cell infiltration differences during wound (Supplementary Figure 6 online); however, "Collagen" downregulation suggests a potential defect in granulation tissue formation. Indeed, this cluster contained MMP family members, suggesting the potential for altered wound matrix remodeling (Figure 4d).

Granulation tissue collagen deposition is perturbed in the wounds of young *PKCα*$^{-/-}$ mice

Given the observed ECM alterations in the *PKCα*$^{-/-}$ mouse skin, and clear differential wound induction of ECM genes in *PKCα*$^{-/-}$ mice, we next asked whether wound matrix deposition would be altered in experimentally induced wounds in young (6 weeks of age) *PKCα*$^{-/-}$ mice. Masson's Trichrome staining revealed a reduced density of newly deposited granulation tissue (Figure 5a and b; day 3 post wounding) and reduced wound collagen content (Figure 5c and d; blue staining; day 7 post wounding). More detailed evaluation of wound collagen content by picrosirius red analysis revealed significantly reduced wound collagen deposition at both 3 and 7 days post wounding. Quantification of newly deposited (fine green/yellow) versus mature (thick red) fibers revealed an initial delay in new fiber deposition (green) on day 3 in PKCα$^{-/-}$ wounds with a subsequent reduction in maturation to thick fibers (red) on day 7. Thus, altered matrix deposition is confirmed as an important aspect of the delayed healing phenotype in *PKCα*$^{-/-}$ mice.

DISCUSSION

Correct production, organization, and maintenance of the dermal ECM are fundamental to the skin's integrity and its ability to repair. Here we show that PKCα deficiency has a profoundly detrimental effect on collagen expression, organization, and function, leading to reduced skin strength and delayed wound healing. Using comprehensive gene expression profiling/clustering, we have identified an

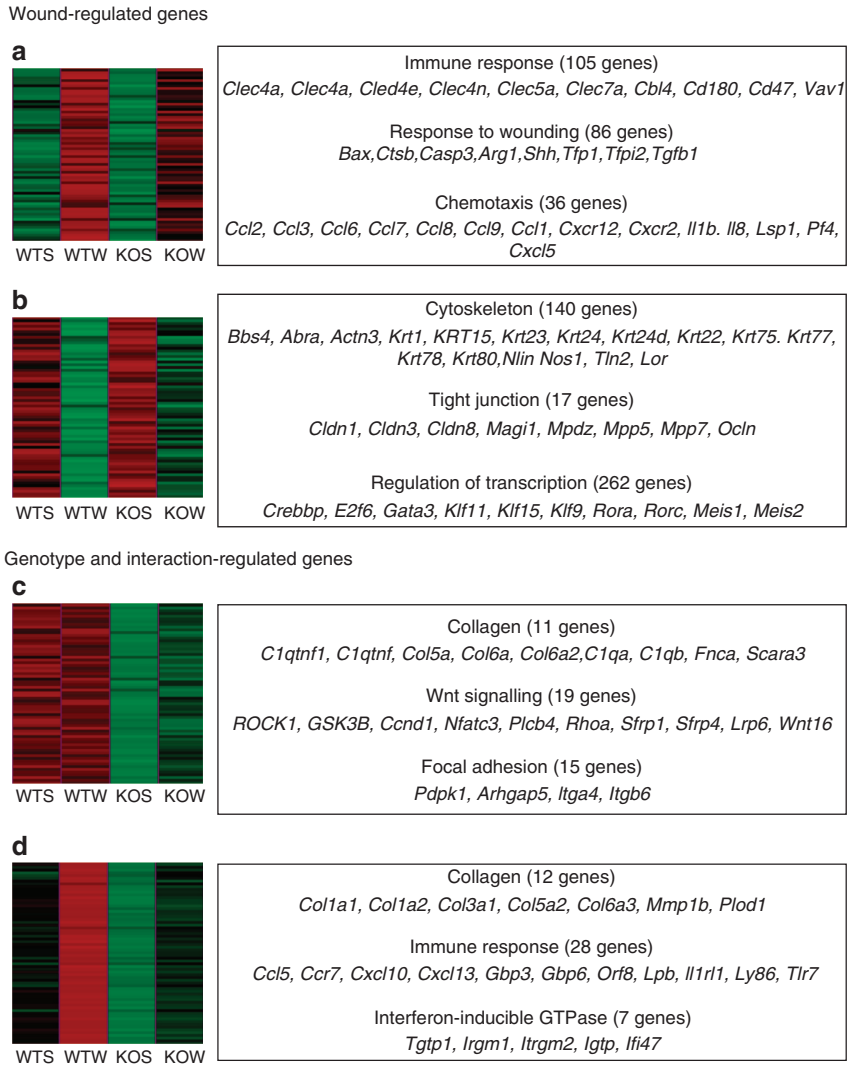

Figure 4. Gene profiling reveals complex expression changes in Knock-out (KO) mice. K-means unsupervised clustering analysis reveals four key patterns of gene expression with associated eisen plots (**a–d**). Analysis revealed genes regulated by wounding alone (**a, b**), genotype alone (**c**), and by interaction between wound and genotype (**d**). Analysis using DAVID identified highly changed gene ontology groups and associated key genes (boxed text) for each cluster. Eisen plots, red, gene induction; green, gene repression. Fold-change > 1.5, $q \leqslant 0.05$. Multiple testing correction Benjamini *P*-value $\leqslant 0.05$ (Gene ontology groups). KOS, knock-out skin; KOW, knock-out wound; WTS, wild-type skin; WTW, wild-type wound. Scale bar = 1 cm.

additional misregulated wound-related process in *PKCα*$^{-/-}$ mice. Collectively, these data reveal that PKCα is essential for efficient and timely wound healing.

Central to skin strength is the supramolecular organization of individual collagen fibrils and the resulting arrangement of dermal collagen bundles (Wess, 2005) known to be regulated, at least in part, by SLRPs (Merline *et al.*, 2009). Here we demonstrate that in the *PKCα*$^{-/-}$ skin both collagen and SLRP family members are reduced at the gene and protein levels, leading to a disordered arrangement of dermal collagen fibrils. These changes have major functional consequences, leading to reduced skin tensile strength, which ultimately results in the development of skin lesions. The ECM phenotype is exaggerated in wound repair with defective granulation tissue deposition in the absence of PKCα. These data, which provide a direct, previously unreported link between PKCα and ECM in the skin, mirror potential roles for PKCα in other tissues, e.g, the kidney (Lee *et al.*, 1999).

The dermal *PKCα*$^{-/-}$ phenotype reported in this study bears a striking resemblance to that previously published for SLRP null mice (Danielson *et al.*, 1997; Chakravarti *et al.*, 1998; Corsi *et al.*, 2002; Tasheva *et al.*, 2002; Nikolovska *et al.*, 2014), in line with reduced SLRP expression in the *PKCα*$^{-/-}$ skin. Increased frequency of larger, irregular collagen fibrils suggests a defect in fibril formation and maturation in the *PKCα*$^{-/-}$ skin. These changes would likely disrupt load transmission from the matrix to collagen fibers (Parkinson *et al.*, 1997) leading to the observed reduction in maximum breaking load. Moreover, despite not reaching statisitical

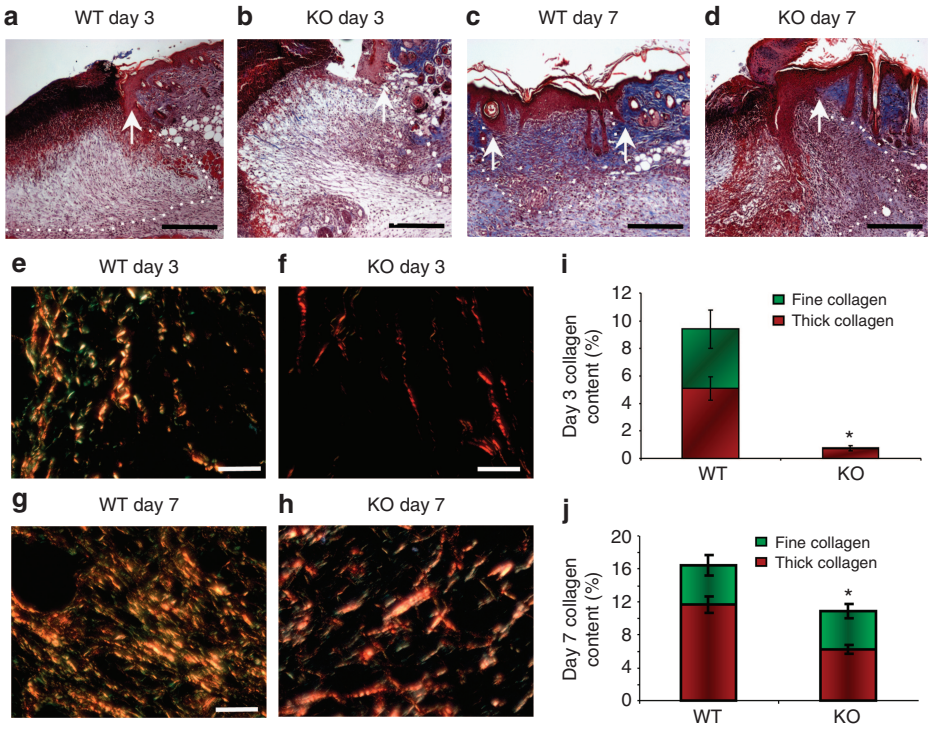

Figure 5. Decreased matrix production in Knock-out (KO) wounds. Masson's Trichrome staining (**a**–**d**) of WT (**a**, **c**) and KO (**b**, **d**) wounds reveals a delay in the replenishment of collagen (blue staining) at both 3 and 7 days post wounding in KO mice. Picrosirius Red staining of the extracellular matrix reveals reduced overall collagen (red/yellow) and reduced newly synthesized collagen (green) at 3 and 7 days post wounding (**e**–**h**) in KO wounds compared with WT wounds. Quantification of collagen content (**i**–**j**). Scale bars = 1 μm (**e**, **g**); *$P < 0.05$, Student's *t*-test based on total collagen content. WT, wild type.

significance, the elastic modulus of the *PKCα*$^{-/-}$ skin was highly variable, implying skin elastic fiber network changes, supported by elastin downregulation in the *PKCα*$^{-/-}$ skin (Table 1).

The precise mechanism by which PKCα alters ECM gene/protein expression remains to be determined. We know that PKCα deficiency leads to reduced expression of the transcription factor Fli1 (Table 1), a known regulator of collagen biosynthesis. Fli1 mutant mice display ultrastructural collagen fibril abnormalities resulting from decreased levels of decorin, fibromodulin, and lumican (Asano *et al.*, 2009). Whereas no published study has linked PKCα to Fli1 activation, PKCδ-mediated phosphorylation of Fli1 in response to TGF-β signaling is vital for correct collagen regulation (Asano and Trojanowska, 2009). Given the numerous examples of parallel regulation and crosstalk between PKCα and PKCδ (Romanova *et al.*, 1998; Lanuti *et al.*, 2006), it seems likely that PKCα also phosphorylates Fli1 in the skin. In an alternative context, PKCα regulates the contractility of cardiac muscle cells by directly phosphorylating fibrous proteins, including the myofibril protein titin, directly increasing fiber tension and stiffness. Intriguingly, titin-based muscle stiffening is a clinical symptom of Ehlers Danlos Syndrome, along with loose skin, abnormal collagen fibril morphology, and irregular wound healing (Hidalgo *et al.*, 2009; Ottenheijm *et al.*, 2012).

Abnormal matrix deposition is a hallmark of all types of chronic non-healing human wounds, often suggested to be the result of decreased fibroblast function combined with increased wound protease activity (Black *et al.*, 2003). We have recently demonstrated that in human chronic wounds keratinocyte PKCα localization is abnormal, leading to functional defects in desmosomal adhesion (Thomason *et al.*, 2012). It is tempting to speculate that altered PKCα may also have an important role in the chronic wound matrix phenotype. Extrapolating our data further, it seems possible that PKCα-mediated alterations to epidermal/dermal architecture may increase the susceptibility of the human skin to injury, with important clinical implications.

MATERIALS AND METHODS

Animal wounding and tissue collection

All animal studies were approved by the UK Government Home Office (Project license 40/3203) following local ethics committee approval. Six-week-old, female, non-littermate PKCα$^{-/-}$ (Leitges *et al.*, 2002)/and WT C57/BL6 mice were anesthetized and wounded (2 × 1 cm full thickness incisions) following our established protocol (Hardman *et al.*, 2008). Wounds were left to heal by secondary intention for 24 hours, and then excised, bisected, and processed for histology or snap-frozen for RNA isolation. For normal skin isolation, 6-week-old, female *PKCα*$^{-/-}$ (Leitges *et al.*, 2002) and WT C57/BL6 mice were killed and their dorsal skin was excised and cut into

1-cm-wide strips for skin tension experiments, fixed for histological processing, or snap-frozen for microarray and protein expression analysis.

Histology and immunohistochemistry

Histological sections were generated from samples fixed in 10% buffered formalin solution and embedded in paraffin wax. Six-micrometer sections from each sample were stained with hemotoxylin and eosin or Masson's Trichrome and images captured using. Fifteen regions were measured from three fields per mouse ($n=7$ WT and 7 *PKCα*$^{-/-}$mice). For picrosirius red staining, sections were incubated in 0.5% Direct red (Sigma-Aldrich, Poole, UK; in saturated picric acid) for 1 hour and visualized using plane-polarized light (Leica, Milton Keynes, UK). Larger, thick collagen fibers appear red, yellow, or orange, and finer fibers appear green. Images were captured using an attached camera (Leica) and ratio of collagen types determined using ImageJ (NIH, Bethesda, MD).

Histology and immunofluorescence

Wound and skin sections were labeled using a polyclonal antibody against Collagen 1 (Millipore, Watford, UK). Bound IgG was detected using the Vectorstain Elite avidin-biotin complex kit (Vector Laboratories, Peterborough, UK) in conjunction with the streptavidin-cy3 complex (Sigma-Aldrich). Control sections treated with PBS instead of polyclonal antibody revealed no signal. Positive Cy3 signal was visualized using a fluorescence microscope (Leica) and attached camera (Coolsnap, Nikon, Kingston-upon-Thames, UK).

Total RNA isolation

Snap-frozen tissue/lysed cells were homogenized for 45 seconds (Ultra Thurrax, IKA, Staufen, Germany) in 1 ml of TriZol reagent (Invitrogen, Paisley, UK). RNA purification was carried out using the Purelink Mini RNA Kit (Ambion, Life Technologies, Paisley, UK) according to the manufacturer's protocol. Purified RNA was resuspended in 30 µl of RNase-free water and was stored at −20 °C.

Microarray analysis

Technical RNA quality was determined using dChip (Li, 2008). Biotinylated cRNA samples were produced from RNA and hybridized to the mouse 430 2.0 oligonucleotide array (Affymetrix, Santa Clara, CA). Background correction, quantile normalization, and gene expression analysis were performed using Robust Multiarray Averaging, followed by principle component analysis (Irizarry *et al.*, 2003). Differential expression between any two comparisons was statistically analyzed using Limma and QVALUE (Smyth 2004) on logarithmic data and differential expression across the full data set was statistically analyzed via two-way ANOVA (Genespring, Agilent Technologies, Santa Clara, CA) on logarithmic data. Two different enriched data sets were generated for analysis using the MaxD visualization software (University of Manchester, UK): (1) differential expression between the normal skin and wound for each genotype with significantly changed probe sets selected on fold change (±1.5), cyberT q-value (<0.05, multiple testing corrected), and expression level in any one array (>50) data presented in Supplementary Tables 4.1–2 and Supplementary Figure 4.2 online); (2) differential expression across the entire data set selected on fold change (±1.5 in any pairwise comparison), any two-dimensional ANOVA q-value (<0.05, multiple testing corrected) and expression level (>50 in any one array), generating a set of 8,378 probe sets (Baldi and Long, 2001). Data were z-transformed and subjected to unsupervised clustering (K-means; MaxD, University of Manchester; data presented in Supplementary Figures 4.3 and Supplementary Table 4.5 online). For each gene set or cluster, over-represented gene ontology groups were identified using the online functional annotation tool in the Database for Annotation, Visualization and Integrated Discovery (DAVID v6.7; Huang da *et al.*, 2007). Significant gene ontology groups were selected on a Benjamimi (false discovery rate) P-value (<0.05). Microarray data have been submitted to ArrayExpress (Accession no. E-MTAB-3836).

Protein extraction and western blotting

Protein from the snap-frozen skin of *PKCα*$^{-/-}$and WT adult mice was extracted using SDS sample buffer, and immunoblotting was performed with 0.2 mg protein. Briefly, samples were separated by denaturing and reducing SDS-PAGE, and were blotted onto 0.2 µm nitrocellulose membrane. Membranes were blocked for 16 hours in Tris-buffered saline (containing 0.1% (v/v) Tween 20) containing 5% (w/v) dry skim milk (Sigma-Aldrich). Primary antibodies raised against Lumican, Decorin and Biglycan (VWR, Abgent) and β-actin (Sigma-Aldrich) were used in conjunction with donkey-anti-rabbit or sheep-anti-mouse secondary antibodies (GE Healthcare, Little Chalfont, UK). Membranes were washed in primary and peroxidase-linked secondary antibodies for 1 hour before probing for antibody binding using ECL Plus detection reagent according to the manufacturer's instructions (GE Healthcare; Gilliver *et al.*, 2010). Quantification of immunoblotting was determined via band area analysis (ImageJ).

Transmission electron microscopy and collagen fibril quantification

Samples were processed as described by Kimura *et al.* (2007), with the exceptions that 4% paraformaldehyde and 2 mM $CaCl_2$ were used in the primary fixative and 2% OsO_4 in the secondary fixative. Twenty digital images of collagen fibrils in a transverse orientation were acquired from each mouse (Gatan Orius CCD SC1000). The diameter of all collagen fibrils within each field of view (20 per mouse) was measured using ImageJ. An average of 800 fibrils were measured per mouse.

Skin tension testing

Age- and hair cycle-matched female mice (four WT and five *PKCα*$^{-/-}$) were shaved and strips of dorsal skin (10 mm × ~30 mm) were excised. Excess fat was removed from the underside of the skin, and tissue was stored in PBS for transportation. Excess PBS was blotted from the skin before tension testing. Course sandpaper was used to hold the skin between clamps attached to a 100-N load cell (Instron, High Wycombe, UK). Each skin sample was loaded to failure at a constant extension rate of 20 mm min^{-1} on an Instron 3344 tension tensing machine (Instron). Tensile strength data were collected using the Bluehill Lite Tension Application Package (Instron). Stress–stress curves were generated and the maximum load (N) at the point of failure was determined.

Non-microarray statistical analysis

All statistical analyses were performed using Prism6 (Graphpad, La Jolla, CA). Individual sideway comparisons were statistically

analyzed using a unpaired *t*-test; multiple comparisons were statistically analyzed by ANOVA, with *post hoc* Tukey's range test. Data distribution in Figure 2d was analyzed using both Kolmogorov–Smirnov and F-tests.

CONFLICT OF INTEREST

The authors state no conflict of interest.

ACKNOWLEDGMENTS

We thank all staff in the University of Manchester Genomic Technologies Facility, particularly Mike Smiga and Andy Hayes for technical assistance. We thank Leo Zeef for bioinformatics and statistical analysis. We thank Stuart Morse and Professor Brian Derby (University of Manchester Material Science) for their invaluable assistance with skin tensile strength measurements. In addition, we thank Samantha Forbes (University of Manchester Electron Microscopy Facility) for assistance with transmission electron microscopy. This work was supported by funding from the Medical Research Council, UK.

SUPPLEMENTARY MATERIAL

Supplementary material is linked to the online version of the paper at http://www.nature.com/jid

REFERENCES

Asano Y, Markiewicz M, Kubo M *et al.* (2009) Transcription factor Fli1 regulates collagen fibrillogenesis in mouse skin. *Mol Cell Biol* 29:425–34

Asano Y, Trojanowska M (2009) Phosphorylation of Fli1 at threonine 312 by protein kinase C delta promotes its interaction with p300/CREB-binding protein-associated factor and subsequent acetylation in response to transforming growth factor beta. *Mol Cell Biol* 29: 1882–94

Baldi P, Long AD (2001) A Bayesian framework for the analysis of microarray expression data: regularized t -test and statistical inferences of gene changes. *Bioinformatics* 17:509–19

Black E, Vibe-Petersen J, Jorgensen LN *et al.* (2003) Decrease of collagen deposition in wound repair in type 1 diabetes independent of glycemic control. *Arch Surg* 138:34–40

Canty EG, Kadler KE (2005) Procollagen trafficking, processing and fibrillogenesis. *J Cell Sci* 118:1341–53

Cataisson C, Pearson AJ, Tsien MZ *et al.* (2006) CXCR2 ligands and G-CSF mediate PKCalpha-induced intraepidermal inflammation. *J Clin Invest* 116: 2757–66

Chakravarti S, Magnuson T, Lass JH *et al.* (1998) Lumican regulates collagen fibril assembly: skin fragility and corneal opacity in the absence of lumican. *J Cell Biol* 141:1277–86

Corsi A, Xu T, Chen XD *et al.* (2002) Phenotypic effects of biglycan deficiency are linked to collagen fibril abnormalities, are synergized by decorin deficiency, and mimic Ehlers-Danlos-like changes in bone and other connective tissues. *J Bone Miner Res* 17:1180–9

Danielson KG, Baribault H, Holmes DF *et al.* (1997) Targeted disruption of decorin leads to abnormal collagen fibril morphology and skin fragility. *J Cell Biol* 136:729–43

Diegelmann RF, Evans MC (2004) Wound healing: an overview of acute, fibrotic and delayed healing. *Front Biosci* 9:283–9

Dissanayake SK, Weeraratna AT (2008) Detecting PKC phosphorylation as part of the Wnt/calcium pathway in cutaneous melanoma. *Methods Mol Biol* 468:157–72

Gilliver SC, Emmerson E, Campbell L *et al.* (2010) 17beta-estradiol inhibits wound healing in male mice via estrogen receptor-alpha. *Am J Pathol* 176: 2707–1

Gordon MK, Hahn RA (2010) Collagens. *Cell Tissue Res* 339:247–57

Hardman MJ, Emmerson E, Campbell L *et al.* (2008) Selective estrogen receptor modulators accelerate cutaneous wound healing in ovariectomized female mice. *Endocrinology* 149:551–7

Hernandez-Maqueda JG, Luna-Ulloa LB, Santoyo-Ramos P *et al.* (2013) Protein kinase C delta negatively modulates canonical Wnt pathway and cell proliferation in colon tumor cell lines. *PLoS One* 8:e58540

Hidalgo C, Hudson B, Bogomolovas J *et al.* (2009) PKC phosphorylation of titin's PEVK element: a novel and conserved pathway for modulating myocardial stiffness. *Circ Res* 105:631–8

Honardoust D, Eslami A, Larjava H *et al.* (2008) Localization of small leucine-rich proteoglycans and transforming growth factor-beta in human oral mucosal wound healing. *Wound Repair Regen* 16:814–23

Honardoust D, Varkey M, Hori K *et al.* (2011) Small leucine-rich proteoglycans, decorin and fibromodulin, are reduced in postburn hypertrophic scar. *Wound Repair And Regen* 19:368–78

Huang, da W, Sherman BT, Tan Q *et al.* (2007) DAVID Bioinformatics Resources: expanded annotation database and novel algorithms to better extract biology from large gene lists. *Nucleic Acids Res* 35: W169–75

Irizarry RA, Hobbs B, Collin F *et al.* (2003) Exploration, normalization, and summaries of high density oligonucleotide array probe level data. *Biostatistics* 4:249–64

Jerome-Morais A, Rahn HR, Tibudan SS *et al.* (2009) Role for protein kinase C-alpha in keratinocyte growth arrest. *J Invest Dermatol* 129:2365–75

Kimura TE, Merritt AJ, Garrod DR (2007) Calcium-independent desmosomes of keratinocytes are hyper-adhesive. *J Invest Dermatol* 127: 775–81

Kimura TE, Merritt AJ, Lock FR *et al.* (2012) Desmosomal adhesiveness is developmentally regulated in the mouse embryo and modulated during trophectoderm migration. *Dev Biol* 369:286–97

Lanuti P, Bertagnolo V, Gaspari AR *et al.* (2006) Parallel regulation of PKC-alpha and PKC-delta characterizes the occurrence of erythroid differentiation from human primary hematopoietic progenitors. *Exp Hematol* 34: 1624–34

Lee HS, Kim BC, Hong HK *et al.* (1999) LDL stimulates collagen mRNA synthesis in mesangial cells through induction of PKC and TGF-beta expression. *Am J Physiol* 277:F369–76

Leitges M, Plomann M, Standaert ML *et al.* (2002) Knockout of PKC alpha enhances insulin signaling through PI3K. *Mol Endocrinol* 16:847–58

Li C (2008) Automating dChip: toward reproducible sharing of microarray data analysis. *BMC Bioinformatics* 9:231

Luna-Ulloa LB, Hernandez-Maqueda JG, Castaneda-Patlan MC *et al.* (2011) Protein kinase C in Wnt signaling: implications in cancer initiation and progression. *IUBMB Life* 63:915–21

Martin P (1997) Wound healing–aiming for perfect skin regeneration. *Science* 276:75–81

Matsui MS, Chew SL, DeLeo VA (1992) Protein kinase C in normal human epidermal keratinocytes during proliferation and calcium-induced differentiation. *J Invest Dermatol* 99:565–71

Merline R, Schaefer RM, Schaefer L (2009) The matricellular functions of small leucine-rich proteoglycans (SLRPs). *J Cell Commun Signal* 3:323–5

Naylor EC, Watson RE, Sherratt MJ (2011) Molecular aspects of skin ageing. *Maturitas* 69:249–56

Nikolovska K, Renke JK, Jungmann O *et al.* (2014) A decorin-deficient matrix affects skin chondroitin/dermatan sulfate levels and keratinocyte function. *Matrix Biol* 35:91–102

Ottenheijm CA, Voermans NC, Hudson BD *et al.* (2012) Titin-based stiffening of muscle fibers in Ehlers-Danlos Syndrome. *J Appl Physiol* 112:1157–65

Parkinson J, Brass A, Canova G *et al.* (1997) The mechanical properties of simulated collagen fibrils. *J Biomech* 30:549–54

Romanova LY, Alexandrov IA, Nordan RP *et al.* (1998) Cross-talk between protein kinase C-alpha (PKC-alpha) and -delta (PKC-delta): PKC-alpha elevates the PKC-delta protein level, altering its mRNA transcription and degradation. *Biochemistry* 37:5558–65

Smyth GK (2004) Linear models and empirical Bayes methods for assessing differential expression in microarray experiments. *Stat Appl Genet Mol Biol* 3:3

Tasheva ES, Koester A, Paulsen AQ *et al.* (2002) Mimecan/osteoglycin-deficient mice have collagen fibril abnormalities. *Mol Vis* 8:407–15

Thomason HA, Cooper NH, Ansell DM *et al.* (2012) Direct evidence that PKCalpha positively regulates wound re-epithelialization: correlation with changes in desmosomal adhesiveness. *J Pathol* 227:346–56

Tibudan SS, Wang Y, Denning MF (2002) Activation of protein kinase C triggers irreversible cell cycle withdrawal in human keratinocytes. *J Invest Dermatol* 119:1282–9

Wallis S, Lloyd S, Wise I *et al.* (2000) The alpha isoform of protein kinase C is involved in signaling the response of desmosomes to wounding in cultured epithelial cells. *Mol Biol Cell* 11:1077–92

Wang HQ, Smart RC (1999) Overexpression of protein kinase C-alpha in the epidermis of transgenic mice results in striking alterations in phorbol ester-induced inflammation and COX-2, MIP-2 and TNF-alpha expression but not tumor promotion. *J Cell Sci* 112:3497–506

Wess TJ (2005) Collagen fibril form and function. *Adv Protein Chem* 70:341–74

Yamanaka O, Yuan Y, Coulson-Thomas VJ *et al.* (2013) Lumican binds ALK5 to promote epithelium wound healing. *PLoS One* 8:e82730

Zeng L, Webster SV, Newton PM (2012) The biology of protein kinase C. *Adv Exp Med Biol* 740:639–1